

Conductivity, NMR Measurements, and Phase Diagram of the $\text{K}_2\text{S}_2\text{O}_7\text{--V}_2\text{O}_5$ System

G. E. Folkmann,[†] K. M. Eriksen,[†] R. Fehrmann,^{*,†} M. Gaune-Escard,[‡] G. Hatem,[‡] O. B. Lapina,[§] and V. Terskikh[§]

Department of Chemistry, Technical University of Denmark, DK-2800 Lyngby, Denmark, Institut Universitaire des Systemes Thermiques Industrielle, Technopole de Chateau-Gombert, rue Enrico Fermi, 5, 13453 Marseille, France, and Boreskov Institute of Catalysis, Prospekt Lavrentiya 5, Novosibirsk 630090, Russia

Received: June 4, 1997; In Final Form: October 6, 1997[⊗]

The phase diagram of the catalytically important $\text{K}_2\text{S}_2\text{O}_7\text{--V}_2\text{O}_5$ system has been investigated by means of conductometric and NMR spectroscopic methods up to 500 °C. From the marked change of the specific conductivity by change of phase, found for 14 different compositions of the $\text{K}_2\text{S}_2\text{O}_7\text{--V}_2\text{O}_5$ binary system, the phase transition temperatures have been obtained. In the V_2O_5 -rich region, where glass formation is pronounced, ^{39}K NMR spectra of six different compositions showed a marked change of the line width at the liquidus temperatures. The phase diagram based on the combined results exhibits three maxima corresponding to the formation of compounds with the stoichiometry $3\text{K}_2\text{S}_2\text{O}_7\cdot\text{V}_2\text{O}_5$, $2\text{K}_2\text{S}_2\text{O}_7\cdot\text{V}_2\text{O}_5$, and $1\text{K}_2\text{S}_2\text{O}_7\cdot\text{V}_2\text{O}_5$ and melting temperatures of 352, 398, and 425 °C, respectively. Three eutectics were found at the compositions $X_{\text{V}_2\text{O}_5} = 0.17, 0.27$, and 0.39 with melting temperatures of 314, 348, and 366 °C, respectively. The measured conductivities in the liquid region of the 14 different compositions have been fitted to polynomials of the form $\kappa = A(x) + B(x)(t - 450) + C(x)(t - 450)^2 + D(x)(t - 450)^3$. The phase diagram may prove to be useful for the design of new SO_2 oxidation catalysts.

Introduction

This paper is a part of a series describing current investigations of the chemistry of molten systems related to the vanadium-based sulfuric acid catalyst, i.e., catalyzing the reaction $\text{SO}_2 + \frac{1}{2}\text{O}_2 \rightleftharpoons \text{SO}_3$. The present paper concerns the phase diagram of the $\text{K}_2\text{S}_2\text{O}_7\text{--V}_2\text{O}_5$ binary system for which conductivity measurements of the liquid system have been performed earlier by us.¹ This system is considered a realistic model system of the catalyst in the oxidized form. Several studies^{2–5} in the past deal with this phase diagram. The great discrepancy among these studies is demonstrated by the published values for the composition of the eutectic, which are 92,² 85,³ 90,⁴ and 78⁵ mol % $\text{K}_2\text{S}_2\text{O}_7$ and the variation in the melting points published for the mixture with $X_{\text{V}_2\text{O}_5} = 0.5$ to be 590,² 490,⁴ and 430⁵ °C, respectively. Even the melting point of the pure component $\text{K}_2\text{S}_2\text{O}_7$ is an object of disagreement. Values such as 415,² 400,⁴ and 420⁵ are reported. Also, the types of compounds claimed to be formed in the binary system are numerous,^{2–7} illustrated by the composition of the claimed compounds having values of the molar ratio $\text{K}_2\text{S}_2\text{O}_7/\text{V}_2\text{O}_5$ equal to 1, 1.25, 1.5, 2, 3, and 6. The reason for this discrepancy may be due to a possible contamination of the hygroscopic melts by water, either during the experiment or by the use of impure $\text{K}_2\text{S}_2\text{O}_7$ contaminated by KHSO_4 , since the previous investigators^{2–5} used $\text{K}_2\text{S}_2\text{O}_7$ made by dehydration of KHSO_4 or by heating commercial products. This usually⁸ leads to a mixture of pyrosulfate and hydrogen sulfate.

Previously, we have constructed the phase diagrams of the analogous catalyst model systems⁹ $\text{Cs}_2\text{S}_2\text{O}_7\text{--V}_2\text{O}_5$ and $\text{M}_2\text{S}_2\text{O}_7\text{--V}_2\text{O}_5$ ($\text{M} = 80\% \text{ K} + 20\% \text{ Na}$)¹⁰ and the $\text{K}_2\text{S}_2\text{O}_7\text{--KHSO}_4$

catalyst solvent system¹¹ by means of conductometric and thermal methods of investigation. In the present $\text{K}_2\text{S}_2\text{O}_7\text{--V}_2\text{O}_5$ system the strong tendency for glass formation has limited the use of conductivity and thermal measurements to obtain phase transition temperatures. However, high-temperature NMR investigations have proven to be very useful for supplementing the conductivity measurements, since the line width changes drastically with phase transitions. The present study is, as far as we know, the first where NMR measurements systematically have been used to construct phase diagrams.

Experimental Section

Chemicals. Since a Raman spectroscopic examination¹² has shown that commercial $\text{K}_2\text{S}_2\text{O}_7$ may contain up to 30% KHSO_4 , $\text{K}_2\text{S}_2\text{O}_7$ was produced by thermal decomposition of $\text{K}_2\text{S}_2\text{O}_8$ (99% from Merck) at 300 °C for about half an hour and under a stream of dry nitrogen to avoid hydrolysis. By Raman spectroscopy, it was proven that $\text{K}_2\text{S}_2\text{O}_7$ produced in this way contained less than 1% K_2SO_4 and KHSO_4 . The V_2O_5 (99.9% from CERAC) was used as obtained.

All manipulations of the chemicals were performed in a glovebox containing dry nitrogen with less than around 5 ppm H_2O .

Conductivity. The electrical conductivity was measured between two fixed electrodes by use of a Radiometer CDM-83 conductivity meter.

The cells used and the calibration procedure have been described elsewhere in detail.¹

Each cell consists of two vertical tubes of borosilicate glass with an inner diameter of 12–17 mm connected to a horizontal capillary tube with a 1 mm inner diameter. The electrodes, which are fused into the bottom of the vertical glass tubes, are made of gold. Gold is the only metal that is completely corrosion resistant to the examined melts. The cells were loaded

[†] Technical University of Denmark.

[‡] Technopole de Chateau-Gombert.

[§] Boreskov Institute of Catalysis.

[⊗] Abstract published in *Advance ACS Abstracts*, November 15, 1997.

in the glovebox and sealed or resealed under oxygen or vacuum. Several investigations^{11–16} have shown that the electrical conductivity of molten salt mixtures in general varies with the temperature after an Arrhenius type law

$$\kappa = A_{\kappa} e^{-E_{\kappa}/(RT)} \quad (1)$$

where κ is the conductivity, A_{κ} is a constant, and E_{κ} is the energy that is necessary for ionic migration from an equilibrium position to a position that allows the ion to cross the potential barrier due to its surroundings.¹⁷ The parameter E_{κ} is therefore dependent on the phase equilibria of the mixture and differs from the solid to the liquid phase. Owing to this fundamental feature, it is possible to determine the temperature of solid–liquid phase transitions by plotting the logarithm of the specific conductivity versus the reciprocal of the absolute temperature. Each straight line region corresponds to a different phase and the intermediate nonlinear region to the solid–liquid two-phase regime. The intersections allow determination of the phase transition temperature for a given composition as shown previously.^{9–11}

NMR Measurements. The ³⁹K NMR spectra were measured on a Bruker MSL-400 spectrometer on natural isotope-containing samples, i.e., containing 93.26% ³⁹K. A frequency of 18.67 MHz, pulse width of 50 μ s, and a delay of 0.15 s between pulses in a 50 kHz frequency range were employed. The chemical shifts were measured relative to the signal from a 0.1 M aqueous KCl solution at room temperature. The home-built high-temperature probe head has been described in detail recently.¹¹ The temperature was measured with an accuracy of 2 °C by a chromel–alumel thermocouple placed 2 mm below the sample. The samples consisted typically of around 3 g of the premelted components sealed in small quartz ampules.¹¹

The used cylindrical furnace has been described in detail elsewhere.¹³ The furnace has a longitudinal region of about 30 cm where the temperature variation is less than 1 °C. An electronic regulation ensures that the temperature variation at a given point in this region is less than 0.1 °C. The temperature was measured with a calibrated chromel–alumel thermocouple.

Results and Discussion

Phase Diagram of the K₂S₂O₇–V₂O₅ System. The conductivity of solid and molten mixtures of 14 different compositions of the K₂S₂O₇–V₂O₅ binary system has been measured at 300–500 °C. The results are shown in Figures 1 and 2 for some compositions as plots of $-\ln(\kappa)$ vs $1/T$. Marked changes of the conductivities are found at temperatures where presumably the phase changes. The mixtures exhibit in several cases large subcooling, and crystallization occurred only after maintaining the cell at a low temperature for many hours. However, for other samples and especially for high mole fractions of V₂O₅, crystallization could not be obtained and the phase transition temperatures could not be identified. This strong tendency for glass formation also made thermal analysis of the phase transition temperatures impossible. Instead, high-temperature ³⁹K NMR measurements were conducted on six different mixtures of the K₂S₂O₇–V₂O₅ system in the temperature range covering the solid and liquid regions. As an example, some of the recorded ³⁹K NMR spectra for the composition $X_{V_2O_5} = 0.33$ are shown in Figure 3. The chemical shift is gradually lowered from around 60 to 0 ppm by stepwise increase of the temperatures from 380 to 400 °C. As can be seen from Figure 4, a plot of the line width vs the temperature for $X_{V_2O_5} = 0.33$ also exhibits a steep drop in the line width in the same temperature

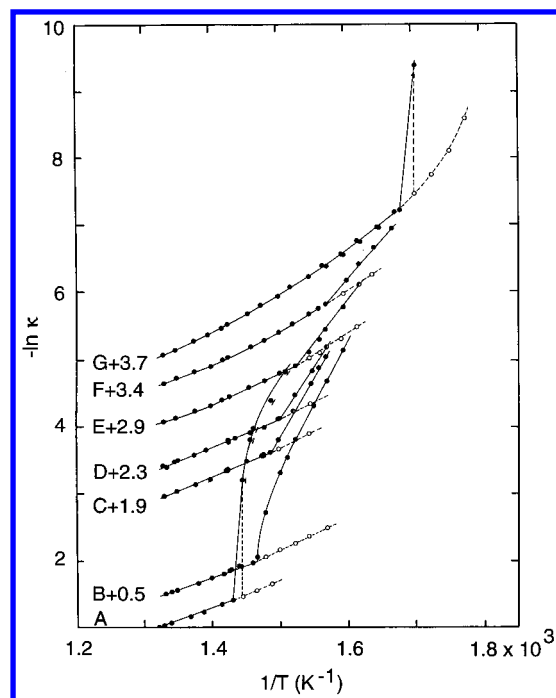


Figure 1. Electric conductivities in the K₂S₂O₇–V₂O₅ system with $-\ln(\kappa)$ vs $1/T$ for the following compositions $X_{V_2O_5}$: A, 0.0000; B, 0.0307; C, 0.0615; D, 0.0803; E, 0.1030; F, 0.1254; G, 0.1738. For clarity the data except those of pure K₂S₂O₇ are offset on the ordinate by the specified values. Open circles indicate subcooling.

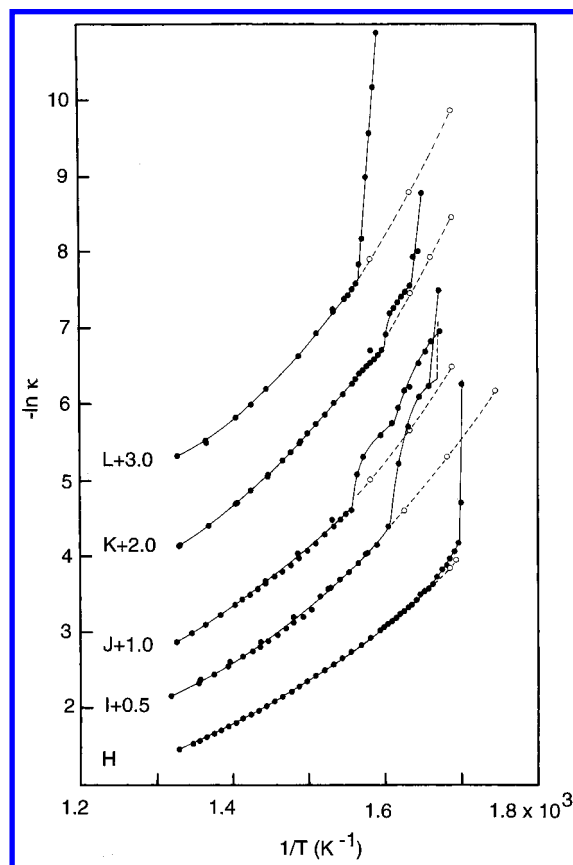


Figure 2. Electric conductivities in the K₂S₂O₇–V₂O₅ system with $-\ln(\kappa)$ vs $1/T$ for the following compositions $X_{V_2O_5}$: H, 0.2001; I, 0.2647; J, 0.3000; K, 0.3704; L, 0.3852. For clarity the data (except composition H) are offset on the ordinate by the specified values. Open circles indicate subcooling.

region followed by a small change at higher temperatures. The same behavior has been observed for the other samples

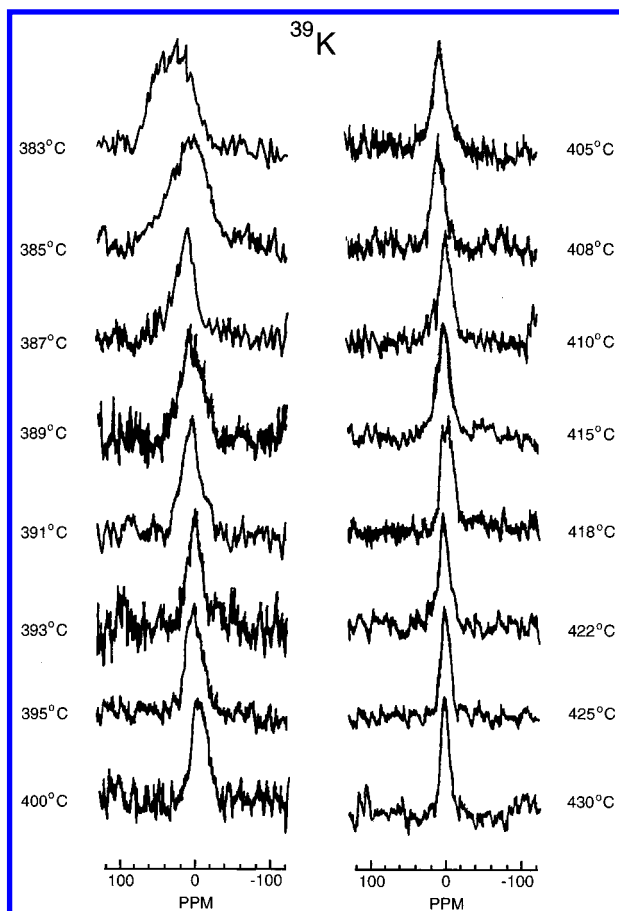


Figure 3. ^{39}K NMR spectra of the $\text{K}_2\text{S}_2\text{O}_7\text{--V}_2\text{O}_5$ system, $X_{\text{V}_2\text{O}_5} = 0.33$, at different temperatures.

measured, and the results for some of them are also displayed in Figure 4. In the solid below the fusion temperature the ^{39}K line is very broad owing to short spin–lattice relaxation. The line width changes drastically by fusion, and the relatively small decrease that proceeds above this temperature is attributed to the decrease in viscosity for these very viscous melts. The phase transition temperatures obtained from both methods of investigation are given in Table 1, and the phase diagram of the $\text{K}_2\text{S}_2\text{O}_7\text{--V}_2\text{O}_5$ system is outlined in Figure 5. For the compositions $X_{\text{V}_2\text{O}_5} = 0.2647$ and 0.3704 the apparent solid-phase transitions found from breaks on the conductivity curves could be due to a change in the solid–gold electrode interface and not to a change of the structure of the solid phase. These transitions are therefore considered less certain and omitted in Figure 5.

The melting temperature of 418°C found for $\text{K}_2\text{S}_2\text{O}_7$ is in excellent agreement with our previous measurements.^{11,18} The phase diagram exhibits most likely three maxima of the compositions $X_{\text{V}_2\text{O}_5} = 0.25$, 0.33 , and 0.50 , respectively. Attempts by ourselves to grow crystals from this system have failed, but previous studies by DTA, IR, and X-ray diffraction^{2–5} have, however, supported the existence of compounds with the stoichiometry $n\text{K}_2\text{S}_2\text{O}_7\cdot\text{V}_2\text{O}_5$, where $n = 1, 2$, or 3 , corresponding to the maxima in Figure 5. Furthermore, in the analogous $\text{Cs}_2\text{S}_2\text{O}_7\text{--V}_2\text{O}_5$ system we have isolated a compound with the stoichiometry $2\text{Cs}_2\text{S}_2\text{O}_7\cdot\text{V}_2\text{O}_5$ corresponding to the maximum at $X_{\text{V}_2\text{O}_5} = 0.33$ found in the $\text{Cs}_2\text{S}_2\text{O}_7\text{--V}_2\text{O}_5$ phase diagram.⁹ Later,¹⁹ by a single-crystal X-ray investigation, this compound was identified as the vanadium (V) dimer $\text{Cs}_4(\text{VO})_2\text{O}(\text{SO}_4)_4$, and probably the analogous compound $\text{K}_4(\text{VO})_2\text{O}(\text{SO}_4)_4$ is also formed, as judged from preliminary X-ray investigations²⁰ on

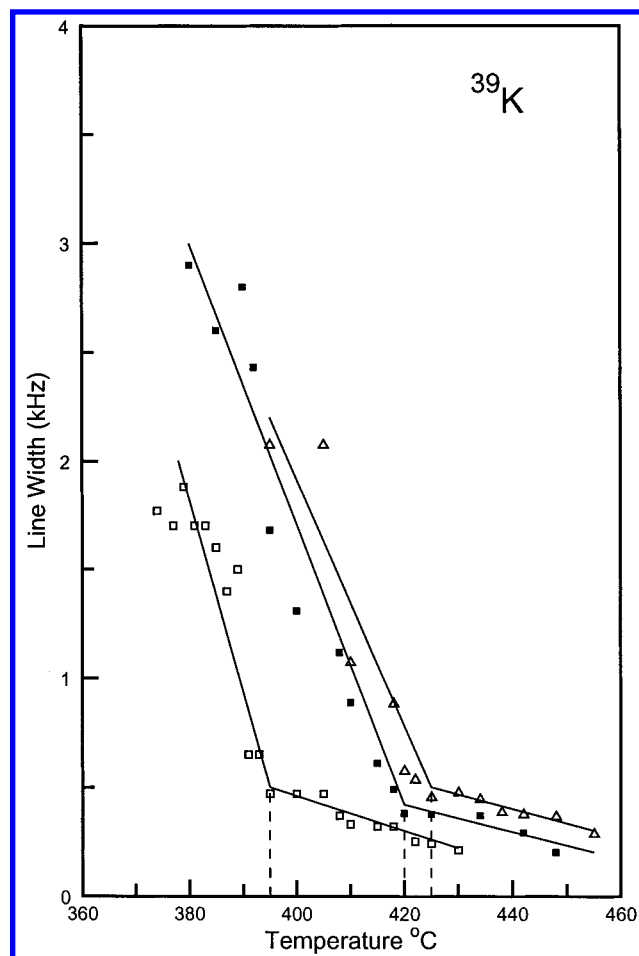


Figure 4. Line width of ^{39}K NMR spectra vs temperature for selected compositions of the $\text{K}_2\text{S}_2\text{O}_7\text{--V}_2\text{O}_5$ system. Values of $X_{\text{V}_2\text{O}_5}$ are as follows: \square , 0.33 ; \blacksquare , 0.44 ; \triangle , 0.50 . Dashed lines indicate phase transition temperatures.

TABLE 1: Conductivity and ^{39}K NMR Measurements of the $\text{K}_2\text{S}_2\text{O}_7\text{--V}_2\text{O}_5$ System: Temperatures ($^\circ\text{C}$) of Transitions

$X_{\text{V}_2\text{O}_5}$	solid phase		fusion of eutectic ^a			liquidus temp	
	transn 1	transn 2	1	2	3	conductivity	NMR
0.0000						419	
0.0307						410	
0.0615						399	
0.0803						394	
0.1030						383	
0.1037			318			378	
0.1254						365	
0.1500			316			324	
0.1738			314				
0.2001			315			329	
0.25							351
0.2647	327 ^b					350	
0.3000				348		369	
0.33							395
0.3704	339 ^b	353 ^b					374
0.38							
0.3852					366		
0.41							386
0.44							409
0.50							423

^a Composition of eutectics 1, 2, and 3 is $X_{\text{V}_2\text{O}_5} = 0.17$, 0.27 , and 0.39 , respectively. ^b Less certain; see text.

crystals very recently obtained from the $\text{K}_2\text{S}_2\text{O}_7\text{--V}_2\text{O}_5$ system. For $X_{\text{V}_2\text{O}_5} = 0.5$ the phase diagram of the $\text{Cs}_2\text{S}_2\text{O}_7\text{--V}_2\text{O}_5$ system also indicates the existence of a compound with the stoichiometry

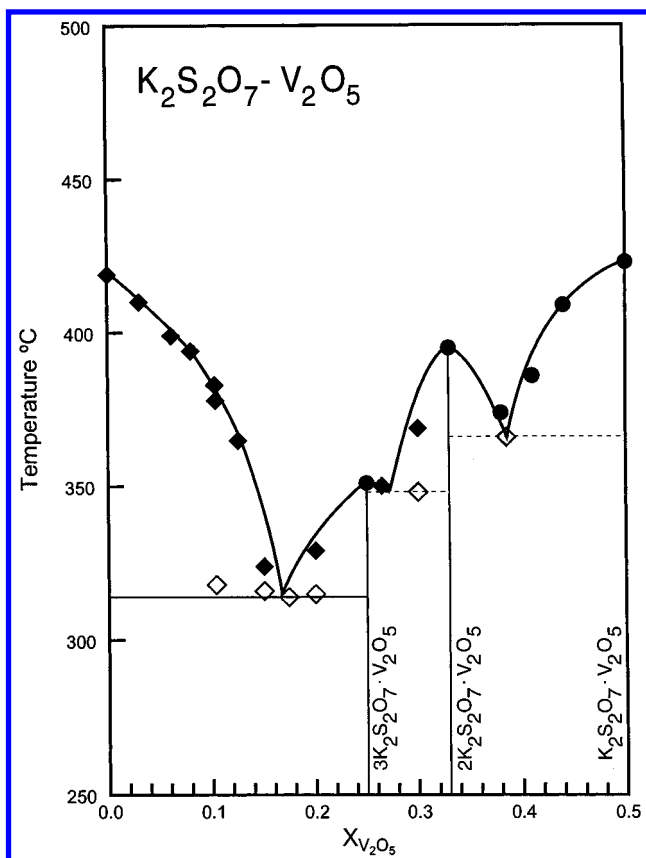


Figure 5. Phase diagram of K₂S₂O₇–V₂O₅ system obtained from conductivity (◆) and ³⁹K NMR spectroscopic measurements (●). Open symbols indicate the melting temperature of a eutectic phase. The compositions of the possible compounds formed in the system are as indicated.

etry Cs₂S₂O₇·V₂O₅, probably formulated as CsVO₂SO₄, as earlier reported²¹ and recently confirmed by ongoing X-ray investigations.²⁰ Therefore, the compound KVO₂SO₄ might possibly also be formed at X_{V₂O₅} = 0.5 in the K₂S₂O₇–V₂O₅ system. The phase diagram of the Cs₂S₂O₇–V₂O₅ system exhibits no maximum at X_{V₂O₅} = 0.25 as in the K₂S₂O₇–V₂O₅ system. A compound with this composition has earlier⁵ been claimed to have the formula K₃VO₂SO₄S₂O₇.

The K₂S₂O₇–V₂O₅ phase diagram in Figure 5 shows three eutectic compositions at around X_{V₂O₅} = 0.17, 0.27, and 0.39 with melting temperatures of 314, 348, and 366 °C, respectively, where the last two are indicated by dashed lines in Figure 5 due to the limited experimental support. Furthermore, the three compounds with the stoichiometry 3K₂S₂O₇·V₂O₅, 2K₂S₂O₇·V₂O₅, and K₂S₂O₇·V₂O₅ melt at 352, 398, and 425 °C, respectively. Previous²² calorimetric measurements point to a steep rise in the liquidus temperature above X_{V₂O₅} = 0.5, presumably up to the melting point of V₂O₅ at 670 °C. Therefore, a eutectic or a peritectic (indicating noncongruent melting of the K₂S₂O₇·V₂O₅ compound) might be found close to X_{V₂O₅} = 0.5. Attempts to calculate the liquidus curve in the composition range 0.5 < X_{V₂O₅} < 1 failed, probably owing to the large deviation from ideality for the molten mixture of V₂O₅ and K₂S₂O₇.

The phase diagrams published so far by others^{2–5} deviate significantly from ours by showing only one eutectic, poorly defined, in the range X_{V₂O₅} = 0.08–0.22 and no maxima but only peritectica compared to our diagram. Also, very large deviations of the liquidus temperatures—up to around 175 °C—are found. This discrepancy is most probably due to the strong tendency for glass formation of the K₂S₂O₇–V₂O₅ binary

TABLE 2: Coefficients for Empirical Equations^a for the Specific Conductivity for Different Compositions X_{V₂O₅} of the Molten K₂S₂O₇–V₂O₅ System^b

X _{V₂O₅}	A(X) Ω ⁻¹ cm ⁻¹ deg ⁻¹	10 ³ B(X) Ω ⁻¹ cm ⁻¹ deg ⁻¹	10 ⁶ C(X) Ω ⁻¹ cm ⁻¹ deg ⁻¹	10 ⁸ D(X) Ω ⁻¹ cm ⁻¹ deg ⁻¹	SD Ω ⁻¹ cm ⁻¹
0.0000	0.294 220	2.1161	1.0445	–6.7150	0.000 00
0.0307	0.269 996	1.4811	45.134	118.34	0.000 18
0.0615	0.248 398	1.6097	44.769	89.099	0.000 19
0.0803	0.233 056	1.5468	44.484	76.322	0.000 25
0.1030	0.221 102	1.7610	44.352	62.030	0.000 20
0.1254	0.198 226	2.1337	43.801	42.860	0.000 31
0.1500	0.230 269	4.3414	64.828	40.264	0.000 05
0.1738	0.269 171	1.6070	–35.188	–27.210	0.002 22
0.2001	0.270 436	4.8321	45.249	18.982	0.010 15
0.2647	0.113 879	1.9756	42.363	35.742	0.000 75
0.3000	0.088 355	1.6926	42.264	39.416	0.000 32
0.3704	0.269 856	6.1190	45.229	11.294	0.032 81
0.3852	0.049 053	1.2763	41.607	40.264	0.000 38

^a $\kappa = A(X) + B(X)(t - 450) + C(X)(t - 450)^2 + D(X)(t - 450)^3$.

^b For the measured temperature ranges, consult Table 1 and Figures 1 and 2.

mixtures. This may lead to vitreous or only partly crystallized samples, which confuse the results of the thermal methods applied in the earlier investigations. In addition—as mentioned in the Introduction—the hygroscopic K₂S₂O₇ used has in several cases most probably been contaminated by water, leading to a partial transformation of K₂S₂O₇ into KHSO₄, affecting the liquidus temperature.

Liquid K₂S₂O₇–V₂O₅ System. As mentioned previously,^{1,22} the conductivity of the liquid region for the measured compositions of the K₂S₂O₇–V₂O₅ system has been fitted to polynomials of the type $\kappa = A(x) + B(x)(t - 450) + C(x)(t - 450)^2 + D(x)(t - 450)^3$. In Table 2 the coefficients are given for the different compositions along with the standard deviations. Satisfactory fits are obtained, since the standard deviations are close to the uncertainty in the measurements of κ . The conductivities obtained here compare well (within ~3%) with those found previously¹ for slightly different compositions.

Relation to Catalysis. The composition range for most commercial SO₂ oxidation catalysts is X_{V₂O₅} = 0.20–0.33. From the phase diagram in Figure 5 it can be seen that the fusion temperature is below 400 °C in this region. If the catalyst melt solidifies in the pores of the solid carrier, the catalyst deactivates. Thus, the catalyst, in its oxidized form (i.e., with vanadium in the +5 oxidation state as in the K₂S₂O₇–V₂O₅ system studied here), may be used at temperatures below 400 °C—even down to 314 °C—if the eutectic composition X_{V₂O₅} = 0.17 proves sufficiently catalytically active. In that case the equilibrium SO₂ + 1/2O₂ ⇌ SO₃ will be shifted so far toward SO₃ that the tail gas contains so little SO₂ that it can be led directly to the atmosphere. Thus, the inconvenient and costly interstage absorption of SO₃ performed in most sulfuric acid plants might be avoided.

Acknowledgment. This investigation has been supported by INTAS (Contract No. 93-3244), BRITE EURAM II (Contract BRE2.CT93.0447), and the Danish Natural Science Research Council.

References and Notes

- (1) Hatem, G.; Fehrmann, R.; Gaune-Escard, M.; Bjerrum, N. J. *J. Phys. Chem.* **1987**, *91*, 195.
- (2) Bazarova, Zh. G.; Boreskov, G. K.; Kefeli, L. M.; Karakchiev, L. G.; Ostankovich, A. A. *Dokl. Akad. Nauk SSSR* **1968**, *180*, 1132.
- (3) Hähle, S.; Meisel, A. *Kinet. Katal.* **1971**, *12*, 1276.

- (4) Maslennikov, B. M.; Illarionov, V. V.; Gubareva, V. N.; Bushuev, N. N.; Tavroskaya, A. Ya.; Leneva, Z. L. *Dokl. Akad. Nauk SSSR* **1978**, 238, 1411.
- (5) Glazyrin, M. P.; Krasil'nikov, V. N.; Ivakin, A. A. *Zh. Neorg. Khim.* **1980**, 25, 3368.
- (6) Borekov, G. K.; Illirionov, V. V.; Ozerov, R. G.; Kil'disheva, E. V. *Zh. Obshch. Khim.* **1954**, 24, 23.
- (7) Gubareva, V. N.; Illiarionov, V. V.; Maslennikov, B. M.; Bushuev, N. N.; Leneva, Z. L.; Mikhailova, I. M.; Vilina, V. Yu.; Krasil'nikova, I. G. *Tr. Nauchn.-Issled. Inst. Udobr. Insektovfungits.* **1977**, 230, 23.
- (8) Fehrmann, R.; Hansen, N. H.; Bjerrum, N. J. *Inorg. Chem.* **1983**, 22, 4009.
- (9) Folkmann, G. E.; Hatem, G.; Fehrmann, R.; Gaune-Escard, M.; Bjerrum, N. J. *Inorg. Chem.* **1991**, 30, 4057.
- (10) Karydis, D. A.; Boghosian, S.; Fehrmann, R. *J. Catal.* **1994**, 145, 312.
- (11) Eriksen, K. M.; Fehrmann, R.; Hatem, G.; Gaune-Escard, M.; Lapina, O. B.; Mastikhin, V. M. *J. Phys. Chem.* **1996**, 100, 10771.
- (12) Hansen, N. H. Ph.D. Thesis, Chemistry Department A, Technical University of Denmark, Lyngby, 1979.
- (13) Andreasen, H. A.; Bjerrum, N. J.; Foverskov, C. E. *Rev. Sci. Instrum.* **1977**, 48, 1340.
- (14) Bloom, H.; Knaggs, I. W.; Molloy, J. J.; Welch, D. *Trans. Faraday Soc.* **1953**, 49, 1458.
- (15) Harrap, B. S.; Heymann, E. *Trans. Faraday Soc.* **1955**, 51, 426.
- (16) Popovskaya, N. P.; Protsenko, P. I. *Zh. Neorg. Khim.* **1962**, 7-9, 2237.
- (17) Morand, G.; Hladik, J. In *Electrochimie des Sels Fondus*; Masson & Co: Paris, 1969; Vol. 1.
- (18) Hansen, N. H.; Fehrmann, R.; Bjerrum, N. J. *Inorg. Chem.* **1982**, 21, 744.
- (19) Nielsen, K.; Eriksen, K. M.; Fehrmann, R. *Inorg. Chem.* **1993**, 32, 4825.
- (20) Nielsen, K.; Eriksen, K. M.; Fehrmann, R. In preparation.
- (21) Glazyrin, M. P.; Krasil'nikov, V. N.; Ivakin, A. A. *Russ. J. Inorg. Chem. (Engl. Transl.)* **1982**, 27, 1740.
- (22) Hatem, G.; Fehrmann, R.; Gaune-Escard, M. *Thermochim. Acta* **1994**, 243, 63.
- (23) Folkmann, G. E.; Hatem, G.; Fehrmann, R.; Gaune-Escard, M.; Bjerrum, N. J. *Inorg. Chem.* **1993**, 32, 1559.